IUST
Iran University of Science and Technology

Iranian Journal of Electrical and Electronic Engineering

Journal Homepage: ijeee.iust.ac.ir

Research Paper

COVID-19 Diagnosis: ULBPFP-Net Approach on Lung Ultrasound Data

V. Esmaeili*, and M. Mohassel Feghhi*(C.A.)

Abstract: The coronavirus disease or COVID-19, as a global disease, is an unprecedented health care crisis due to increasing mortality and its high rate of infection. Patients usually show significant complications in the respiratory system. This disease is caused by SARS-CoV-2. Decreasing the time of diagnosis is essential for reducing deaths and low spreading of the virus. Also, using the optimal tool in the pediatric setting and Intensive care unit (ICU) is required. Therefore, using lung ultrasound is recommended. It does not have any radiation and it has a lower cost. However, it makes noisy and low-quality data. In this paper, we propose a novel approach called Uniform Local Binary Pattern on Five intersecting Planes and convolutional neural Network (ULBPFP-Net) that overcomes the said limitation. We extract worthwhile features from five planes for feeding a network. Our experiments confirm the success of the ULBPFP-Net in COVID-19 diagnosis compared to the previous approaches.

Keywords: COVID-19, Convolutional Neural Network, ULBPFP-Net, Lung Ultrasound Images.

1 Introduction

THE COVID-19 represents a pandemic disease challenge [1]. So it is an unprecedented health care crisis due to increasing mortality and its high rate of infection [2, 3]. This newly discovered disease is caused by the third pathogenic human coronavirus, i.e., SARS-CoV-2 [4, 5]. As of today, July 6, 2022, a total of 548,990,094 COVID-19 confirmed cases and 6,341,637 deaths have been reported worldwide according to the WHO. This disease was first hit the China in 2019 [6]. Next, it has spread quickly worldwide from 2020 [7].

Iranian Journal of Electrical and Electronic Engineering, 2023.
Paper first received 08 Jul 2022, revised 10 May 2023, and accepted 12 May 2023.
*The authors are with Faculty of Electrical and Computer Engineering, University of Tabriz, Tabriz, Iran.
E-mails: v.esmaeili@tabrizu.ac.ir, and mohasselfeghhi@tabrizu.ac.ir.
Corresponding Author: M. Mohassel Feghhi.
https://doi.org/10.22068/IJEEE.19.3.2612.

The visual appearance of the virus under an electron microscope to solar corona is the cause of its name [8]. 20% of patients show serious and important complications to the respiratory system, and the other 80% have mild symptoms [9]. Usually, the patients are admitted to the emergency department with fever > 37.5 °C, dry cough, respiratory symptoms, gastrointestinal symptoms, asthenia, dyspnea, sore throat, headache, and myalgia [10, 11]. This infection has severe pulmonary involvement [11].

The RT-PCR is a method for molecular identify based on the detection of viral RNA [1, 11]. However, its result is sometimes available after twenty-four hours [7]. Decreasing the time of diagnosis is essential for reducing deaths and low spreading of the virus. The false-negative rate of this test is 30% [1, 12]. Thus, its accuracy is unclear [1].

If the RT-PCR is negative, then Computed Tomography (CT) scan is useful [1]. This first-line imaging is considered the most accurate and rapid

mode to evaluate patients [13]. Nonetheless, it has the disadvantages of the high workload of scanner cleaning and large radiation exposure. Also, it is a suboptimal option in the pediatric setting, and it is not universally available [11, 13, 14].

Chest X-ray provides a 2-dimensional image of the lung. Its advantages are low radiation exposure, low cost, fast, and wide availability. Nevertheless, it has less sensitivity than the CT scan [11]. Moreover, diagnostic imaging staff and uninfected patients may are put at risk of disease transmission when taking chest X-rays through contaminated surfaces [15].

Therefore, lung ultrasound is recommended as an alternative. Because it does not have any radiation and it has a lower cost. Furthermore, contamination risk is lower using it. This safe imaging has high diagnostic accuracy and sensitivity in comparison with CT [11]. In addition, its findings have concordance with X-ray in most COVID-19 cases [16]. Hence, using it makes a significant interest. Even, it is used as an important tool in affected children [16-18]. If the disease is in the early phases, it is possible to determine lung involvement using ultrasound [5]. These advantages have made ultrasound striking [19-21].

However, there are limited COVID-19 studies on ultrasound. One of the reasons is the noisy and low quality of images in ultrasound data [22]. Thus, researchers have applied wavelet transformation and noise filtering for ultrasound data improvement in quality [22, 23]. Reducing unwanted noise and selecting a suitable model can provide superior COVID-19 detection accuracy on ultrasound images against other data [22].

The other reason is the lack of a large and balanced ultrasound dataset containing hundreds of patients [24]. Perhaps, less recorded data is due to less established practice using ultrasound for examining COVID-19 [8]. A large and available dataset will be necessary for the development of deep learning techniques. It makes reliable the validation of any automated COVID-19 diagnostic tool. Besides, some techniques such as reflection, resizing, and rotation can apply for data augmentation. Also, utilizing a pre-trained model is beneficial.

With the quick development of the disease, ever more data and machine learning techniques with promising performances are required to diagnose COVID-19. Because interpretation of data is operator-dependent and time-consuming [25]. Thus, spotting and classification of the disease using ultrasound data and artificial intelligence is attention nowadays [22, 24, 26]. Nonetheless, it is nice the combination of a pre-trained model and a handcrafted method that takes meaningful characteristics.

Ergo, we propose a new ULBPFP-Net approach in this paper. We extract worthwhile features from five proposed planes for feeding a network. The five planes can provide beneficial information on the disease's appearance in ultrasound data. It produces successfulness in COVID-19 diagnosis.

The main contributions of the model proposed in this paper are as follows:

i) The combination of the pre-trained VGG and a handcrafted method to take meaningful features.

ii) Proposing a novel ULBPFP-Net method, which is robust to the noise.

iii) Extracting the features from five proposed planes for feeding a network.

2 Related Works

The machine learning techniques supply a fast understanding of critically ill patients' situations [22]. A classifier network has been suggested based on the disease biomarkers on ultrasound data in 2020 [26]. The network is obtained from spatial transformer networks. It predicts the intensity of the disease according to the input frame. However, the used labeled dataset was limited. The labels indicate disease degrees.

Then, the VGG19 model is selected by Horry *et al.* [22]. They have shown that the optimized model can be used for the highly scarce dataset. The achieved precision was 100% for ultrasound, 86% for X-ray, and 84% for CT data. Also, both confusion matrix and training curves for ultrasound experiments were near to ideal. It is specified that although ultrasound images are noisy and difficult to interpret by the untrained eye, a pre-trained network is executable for them.

The work [27] proposes a deep CNN called POCOVID-Net on 3-class POCUS. The accuracy is reported at 89% using this method for detecting COVID-19, whereas it is 87% in the extended work [28]. In [24], pre-trained CNN models have been adapted on POCUS [27]. This dataset comprises 3326 frames of ultrasound. The best achieved average accuracy is 89.1% by using the InceptionV3 network for COVID-19 detection in [24]. Furthermore, the LUSNet [29] approach has been proposed to classify lung ultrasound data. This

approach uses U-Net [30]. Its average accuracy has been confirmed at 97%.

To stratify the disease indications, a lightweight network is presented in [25]. In fact, MobileNets [31] have been utilized on the ultrasound dataset in this work [25]. All videos were collected from GrepMed, Butterfly iQ, EMCrit project, POCUS Atlas, and Twitter sources. They were annotated by a junior and a senior radiologist. The achieved accuracy was above 95% using the MobileNet. Nonetheless, using beneficial planes can describe the texture skillfully [32-40]. The planes' information can combine with a network.

3 The proposed ULBPFP-Net Method

In this paper, we aim to release the limitations and increase the accuracy. Hence, we propose a novel method named ULBPFP-Net. Since it is resistant to noise, it has high skillfulness in ultrasound images analysis. Also, it extracts worthwhile features using five proposed planes.

Suppose the ultrasound data are sequential images received from the ultrasound video. We line them up one after the other (see Fig. 1). Then, the five planes hold the ultrasound images' pixels to carry out the ULBP (β) (Fig. 1). For defining the five planes, if the width, height, and length of the sequential ultrasound images are W, H, L, respectively then, the coordinate of held pixels per plane are as follows:

$$(W\mu + cos(k), H\mu - sin(k), L\mu) \quad (1)$$

$$(W\mu + cos(k), H\mu, L\mu + sin(k)) \quad (2)$$

$$(W\mu - cos(k), H\mu - sin(k), L\mu - sin(k)) \quad (3)$$

$$(W\mu, H\mu - sin(k), L\mu + cos(k)) \quad (4)$$

$$(W\mu + cos(k), H\mu - sin(k), L\mu + sin(k)) \quad (5)$$

where per equation belongs to the plane with its number. The k is $2\pi\tau/\rho$. If there are ρ=4 pixels around the midst pixel, then the coordinate of the pixels in the yellow plane (see Fig. 1) is achieved by Equation (2) as shown in Fig. 2. The ULBPFP ($Fi\beta$) feature is achieved as below:

$$\vartheta\beta = \begin{cases} \sum_{j=1}^{\rho} \zeta(\propto_\tau - \mu) & if\ \beta \le 2 \\ \rho + 1 & O/W \end{cases} \quad (6)$$

$$Fi\beta = [\vartheta\beta_1; \dots; \vartheta\beta_5]$$

$$\zeta(\propto_j - \mu) = \begin{cases} 1 & \propto_j \ge \mu \\ 0 & \propto_j < \mu \end{cases} \quad (7)$$

$$\beta = |\zeta(\propto_\tau - \mu) - \zeta(\propto_1 - \mu)| + \sum_{j=1}^{\rho} |\zeta(\propto_j - \mu) - \zeta(\propto_{j-1} - \mu)| \quad (8)$$

where ϑ means histogram. The around pixels and their number are $\propto and\ \tau$. A pixel (μ) is in their midst. ζ is the sign.

In fact, the pixel values are minus the μ value. If the result is positive, then "1" is replaced and otherwise "0" is put. These "0" and "1" are concatenated together (for example, 01100001).

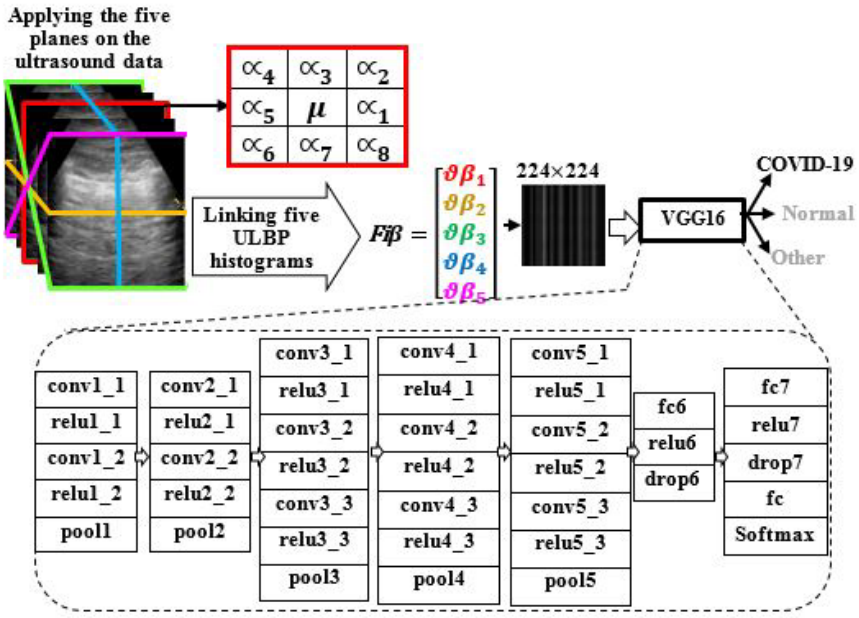

Fig. 1 The proposed ULBPFP-Net method on the ultrasound data.

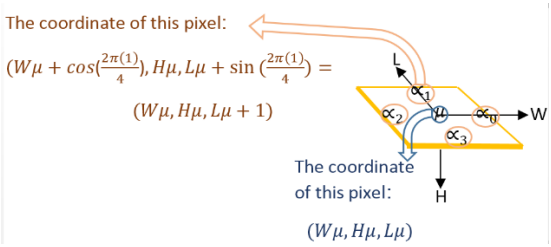

Fig. 2 The coordinates of pixels in the yellow plane.

If the number of transitions between 1 and 0 is less than 2, then it is placed into a uniform bin. A distinct bin contains others. Finally, the obtained results from 5 planes are inserted in a matrix named $Fi\beta$.

The motivation of using the five planes is data consistency for training a very deep convolutional network with only relevant extracted features. In fact, these five planes may provide beneficial information on the disease's appearance in images.

The $Fi\beta$ matrix is resized to 224×224 for preparing pre-trained VGG16 input. The VGG16 [41] has a 16-depth weight layer with very small 3×3 convolution filters. We use it due to provide suitable results within the limitations during the initial model selection experiments in [22]. Although it maintains original layers and weights, the last three layers are exchanged for classifying COVID-19 and others. Thus, it would be able to generalize and converge by training with low tagged data.

A solver is determined for VGG16 training. Also, the most number of periods training the $Fi\beta$s is defined as max epochs. Mini-batch size and validation frequency are used per iteration. Finally, the VGG16 will classify the input data with the predicted class labels. Fig. 1 shows our proposed ULBPFP-Net method on the ultrasound data.

4 Experiments, Evaluation, and Comparison

We use MATLAB 2020 for our purpose implementation. The available ultrasound data are taken from https://github.com/jannisborn/covid19_ultrasound [27]. It contains one hundred fifteen COVID-19, seventy-five normal, and fifty-seven other lung disease videos.

The frames put as a line one after the other. The five planes hold the pixels. The ULBP carries out comparing around and medial pixel quantity. Linking its histograms together makes the ULBPFP ($Fi\beta$) matrix. It is resized to 224×224.

Now, the matrix is prepared for pre-trained VGG16. Each matrix and its label (COVID-19, normal, or other) is given to the VGG16. Thus, the VGG16 learns relevant features to the disease's appearance. Finally, it can classify them in case 3 categories after 70% training random input data, skillful.

Layers transfer is done for the last layers. The stochastic gradient descent optimizing algorithm is utilized for updating the biases and weights to minimize the loss function. Max epochs and validation frequency are 30. The mini-batch size and initial learning rate are 16 and 1e-6, individually. We note that the two last options influence accuracy results. The effect of the mini-batch size and learning rate choosing on the disease diagnosis accuracy is depicted in Fig. 3.

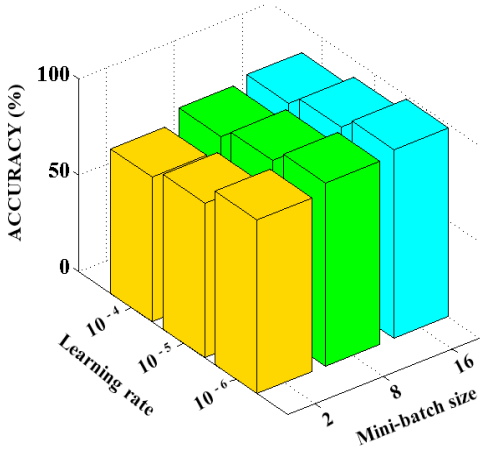

Fig. 3 The effects of the mini-batch size and learning rate choosing on the accuracy.

Fig. 4 shows learning curves for the ultrasound experiment. The training curves are near to ideal. The average accuracy is 98% using our ULBPFP-Net method for COVID-19 detection.

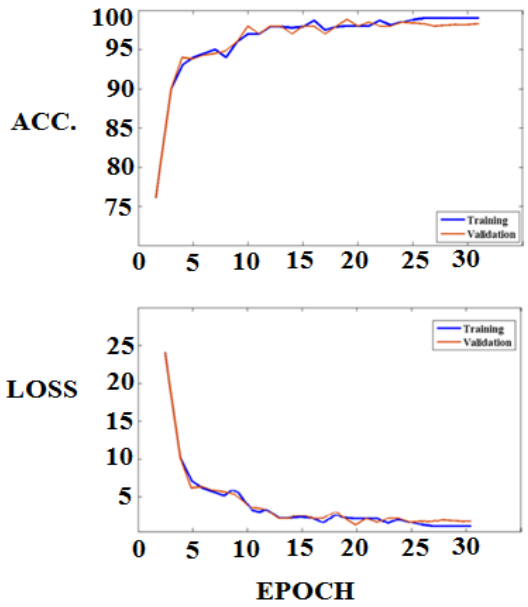

Fig. 4 Learning curves for the ultrasound data.

Fig. 5 displays the ROC curve for COVID-19, normal, and other classes. The best sensitivity are 99.2%, 99%, and 98.5% for COVID-19, other, and normal, respectively. For further analysis, we compute the F1 score (F), precision (P), and specificity (S) as follows [42]:

$$F = 2\left(\frac{P\times\frac{\xi}{\xi+false\,neg.}}{P+\frac{\xi}{\xi+false\,neg.}}\right) \quad (9)$$

$$P = \frac{\xi}{\chi+\xi} \quad (10)$$

$$S = \frac{\eta}{\eta+\chi} \quad (11)$$

where χ, ξ, $and\ \eta$ are false positive, true pos., and true negative. Table 1 illustrates the performance of the ULBPFP-Net. The results confirm the extraction of worthwhile features using five proposed planes. Most importantly, COVID-19 can be distinguished best with a precision of 100%. Table 2 compares the precision in our and other works. In fact, it indicates correct predictions. Table 3 compares the ULBPFP-Net with the other state-of-the-art. It demonstrates the successfulness of the ULBPFP-Net. Besides, the computational time for training of different methods is shown in Fig. 6.

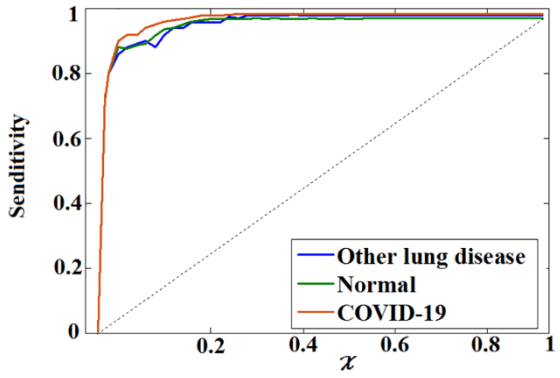

Fig. 5 ROC curve for COVID-19, normal, and other classes. The false-positive rate is indicated by χ.

Table 1 The performance of the ULBPFP-Net.

Class	F	P	S
Normal	0.98	0.99	0.96
COVID-19	0.99	1.00	0.98
Other	0.99	0.99	0.99

5 Conclusion

The ULBPFP-Net is suggested for COVID-19 diagnosis on ultrasound data in this paper. In this approach, the matrix of linked ULBP histograms from five planes is fed to VGG16. Its advantages are increasing the diagnosis rate in ultrasound data, robustness to noise, and overcoming low data problems. The used network profits the feature of five planes. These five planes are in line with the appearance of COVID-19 in the ultrasound texture. Hence, they can reveal lung diseases such as COVID-19, carefully.

Table 2 Comparing the precision in our and other works.

Class	Work	Precision
COVID-19	POCOVID-Net [27]	87%
	InceptionV3 [24]	90%
	VGG19 [22]	86%
	ULBPFP-Net (our work)	**100%**
Normal	POCOVID-Net [27]	89%
	InceptionV3 [24]	92%
	VGG19 [22]	89%
	ULBPFP-Net (our work)	**99%**
Other	POCOVID-Net [27]	83%
	InceptionV3 [24]	84%
	VGG19 [22]	81%
	ULBPFP-Net (our work)	**99%**

Table 3 Comparing the ULBPFP-Net with the other state-of-the-art

Work	Accuracy
[22]	86%
[25]	95%
[26]	96%
[27]	89%
[29]	97%
[39]	98.5%
[40]	98.7%
Our ULBPFP-Net	**99%**

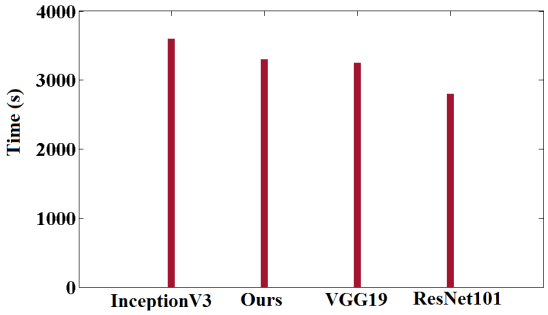

Fig. 6 The computational time for training of different methods.

Intellectual Property

The authors confirm that they have given due consideration to the protection of intellectual property associated with this work and that there are no impediments to publication, including the timing to publication, with respect to intellectual property.

Funding

No funding was received for this work

Credit Authorship Contribution Statement

V. Esmaeili: Idea & Conceptualization, Research & Investigation, Data Curation, Analysis, Methodology, Software and Simulation, Original Draft Preparation. **M. Mohassel Feghhi:** Analysis, Methodology, Project Administration, Supervision, Data Curation, Verification, Revise & Editing

Declaration of Competing Interest

The authors hereby confirm that the submitted manuscript is an original work and has not been published so far, is not under consideration for publication by any other journal and will not be submitted to any other journal until the decision will be made by this journal. All authors have approved the manuscript and agree with its submission to "Iranian Journal of Electrical and Electronic Engineering".

References

[1] C. Sorlini *et al.*, "The role of lung ultrasound as a frontline diagnostic tool in the era of COVID-19 outbreak," *Internal and emergency medicine*, Vol. 16, No. 3, pp. 749-756, 2021.

[2] Y. Zhang, H. Xue, M. Wang, N. He, Z. Lv, and L. Cui, "Lung ultrasound findings in patients with coronavirus disease (COVID-19)," *American Journal of Roentgenology*, Vol. 216, No. 1, pp. 80-84, 2021.

[3] L. Gargani, H. Soliman-Aboumarie, G. Volpicelli, F. Corradi, M. C. Pastore, and M. Cameli, "Why, when, and how to use lung ultrasound during the COVID-19 pandemic: enthusiasm and caution," *European Heart Journal-Cardiovascular Imaging*, Vol. 21, No. 9, pp. 941-948, 2020.

[4] S. Bar *et al.*, "The association of lung ultrasound images with COVID-19 infection in an emergency room cohort," *Anaesthesia*, Vol. 75, No. 12, pp. 1620-1625, 2020.

[5] C. McDermott, M. B. Lacki, B. Sainsbury, J. Henry, M. Filippov, and C. Rossa, "Sonographic diagnosis of COVID-19: A review of image processing for lung ultrasound," *Frontiers in big Data*, Vol. 4, p. 2, 2021.

[6] G. Secco *et al.*, "Lung ultrasound presentation of COVID-19 patients: phenotypes and correlations," *Internal and Emergency Medicine*, Vol. 16, pp. 1317-1327, 2021.

[7] N. Buda, E. Segura-Grau, J. Cylwik, and M. Wełnicki, "Lung ultrasound in the diagnosis of COVID-19 infection-A case series and review of the literature," *Advances in medical sciences*, Vol. 65, No. 2, pp. 378-385, 2020.

[8] A. Ulhaq, J. Born, A. Khan, D. P. S. Gomes, S. Chakraborty, and M. J. I. A. Paul, "Covid-19 control by computer vision approaches: A survey," *Advances in medical sciences*, Vol. 8, pp. 179437-179456, 2020.

[9] F. Mento *et al.*, "Deep learning applied to lung ultrasound videos for scoring COVID-19 patients: A multicenter study," *The Journal of the Acoustical Society of America*, Vol. 149, No. 5, pp. 3626-3634, 2021.

[10] G. Volpicelli *et al.*, "Lung ultrasound for the early diagnosis of COVID-19 pneumonia: an international multicenter study," *Intensive care medicine*, vol. 47, no. 4, pp. 444-454, 2021.

[11] L. R. Sultan, C. Sehgal, "A review of early experience in lung ultrasound in the diagnosis and management of COVID-19," *Ultrasound in Medicine & Biology*, Vol. 46, No. 9, pp. 2530-2545, 2020.

[12] T. Ai *et al.*, "Correlation of chest CT and RT-PCR testing for coronavirus disease 2019 (COVID-19) in China: a report of 1014 cases," *Radiology*, Vol. 296, No. 2, pp. E32-E40, 2020.

[13] D. Colombi *et al.*, "Comparison of admission chest computed tomography and lung ultrasound performance for diagnosis of COVID-19 pneumonia in populations with different disease prevalence," *European journal of radiology*, Vol. 133, p. 109344, 2020.

[14] M. Allinovi *et al.*, "Lung ultrasound may support diagnosis and monitoring of COVID-19 pneumonia," *Ultrasound in Medicine and Biology*, Vol. 46, No. 11, pp. 2908-2917, 2020.

[15] E. M. Chamorro, A. D. Tascón, L. I. Sanz, S. O. Vélez, and S. B. J. R. Nacenta, "Radiologic diagnosis of patients with COVID-19,"

Radiología (English Edition), Vol. 63, No. 1, pp. 56-73, 2021.

[16] M. Denina *et al.*, "Lung ultrasound in children with COVID-19," *Pediatrics*, vol. 146, no. 1, 2020.

[17] A. M. Musolino *et al.*, "Lung ultrasound in children with COVID-19: preliminary findings," *Ultrasound in medicine & biology*, Vol. 46, No. 8, pp. 2094-2098, 2020.

[18] X. Qian *et al.*, "Current ultrasound technologies and instrumentation in the assessment and monitoring of COVID-19 positive patients," *IEEE transactions on ultrasonics, ferroelectrics, and frequency control*, Vol. 67, No. 11, pp. 2230-2240, 2020.

[19] M. J. Fiala, "A brief review of lung ultrasonography in COVID-19: is it useful?," *Annals of emergency medicine*, vol. 75, no. 6, pp. 784-785, 2020.

[20] J. C.-H. Cheung and K. N. Lam, "POCUS in COVID-19: pearls and pitfalls," *The Lancet Respiratory Medicine*, Vol. 8, No. 5, p. e34, 2020.

[21] E. Poggiali *et al.*, "Can lung US help critical care clinicians in the early diagnosis of novel coronavirus (COVID-19) pneumonia?," *Radiology*, vol. 295, no. 3, pp. E6-E6, 2020.

[22] M. J. Horry *et al.*, "COVID-19 detection through transfer learning using multimodal imaging data," *IEEE Access*, Vol. 8, pp. 149808-149824, 2020.

[23] P. Singh, R. Mukundan, and R. De Ryke, "Feature enhancement in medical ultrasound videos using contrast-limited adaptive histogram equalization," *Journal of digital imaging*, Vol. 33, No. 1, pp. 273-285, 2020.

[24] J. Diaz-Escobar *et al.*, "Deep-learning based detection of COVID-19 using lung ultrasound imagery," *Plos one*, Vol. 16, No. 8, p. e0255886, 2021.

[25] A. Almeida *et al.*, "Lung ultrasound for point-of-care COVID-19 pneumonia stratification: computer-aided diagnostics in a smartphone. First experiences classifying semiology from public datasets," in *2020 IEEE International Ultrasonics Symposium (IUS)*, pp. 1-4: IEEE, 2020.

[26] S. Roy *et al.*, "Deep learning for classification and localization of COVID-19 markers in point-of-care lung ultrasound," *IEEE transactions on medical imaging*, Vol. 39, No. 8, pp. 2676-2687, 2020.

[27] J. Born *et al.*, "POCOVID-Net: automatic detection of COVID-19 from a new lung ultrasound imaging dataset (POCUS)," *arXiv preprint arXiv:2004.12084*, 2020.

[28] J. Born *et al.*, "Accelerating detection of lung pathologies with explainable ultrasound image analysis," *Applied Sciences*, Vol. 11, No. 2, p. 672, 2021.

[29] M. R. Panicker, Y. T. Chen, K. V. Narayan, C. Kesavadas, and A. Vinod, "An approach towards physics informed lung ultrasound image scoring neural network for diagnostic assistance in COVID-19," *arXiv preprint arXiv:2106.06980*, 2021.

[30] O. Ronneberger, P. Fischer, and T. Brox, "U-net: convolutional networks for biomedical image segmentation," in *International Conference on Medical image computing and computer-assisted intervention*, pp. 234-241, 2015.

[31] A. G. Howard *et al.*, "Mobilenets: efficient convolutional neural networks for mobile vision applications," *arXiv preprint arXiv:1704.04861*, 2017.

[32] V. Esmaeili, M. M. Feghhi, and S. O. Shahdi, "Automatic micro-expression apex frame spotting using local binary pattern from six intersection planes," *arXiv preprint arXiv: 2104.02149*, 2021.

[33] G. Zhao, and M. Pietikainen, "Dynamic texture recognition using local binary patterns with an application to facial expressions," *IEEE transactions on pattern analysis and machine intelligence*, Vol. 29, No. 6, pp. 915-928, 2007.

[34] V. Esmaeili, M. M. Feghhi, and S. O. Shahdi, "Autonomous apex detection and micro-expression recognition using proposed diagonal planes," *International Journal of Nonlinear Analysis and Applications*, Vol. 11, pp. 483-497, 2020.

[35] V. Esmaeili, and S. O. Shahdi, "Automatic micro-expression apex spotting using Cubic-

LBP," *Multimedia Tools and Applications*, Vol. 79, No. 27, pp. 20221-20239, 2020.

[36] V. Esmaeili, M. M. Feghhi, and S. O. Shahdi, "Micro-expression recognition using histogram of image gradient orientation on diagonal planes," In *2021 5th International Conference on Pattern Recognition and Image Analysis (IPRIA)*, pp: 1-5, IEEE, 2021.

[37] V. Esmaeili, M. Mohassel Feghhi, and S. O. Shahdi, "A comprehensive survey on facial micro-expression: approaches and databases," *Multimedia Tools and Applications*, Vol. 81, No. 18, 2022.

[38] V. Esmaeili, M. Mohassel Feghhi, and S. O. Shahdi, "Micro-expression recognition based on the multi-color ULBP and histogram of gradient direction from six intersection planes," *Journal of Iranian Association of Electrical and Electronics Engineers*, 2022.

[39] V. Esmaeili, and M. Mohassel Feghhi, "Diagnosis of Covid-19 disease by combining hand-crafted and deep-learning methods on ultrasound data," *Journal of Machine Vision and Image Processing*, Vol. 9, No. 4, 2022.

[40] V. Esmaeili, M. M. Feghhi, and S. O. Shahdi, "Early COVID-19 diagnosis from lung ultrasound images combining RIULBP-TP and 3D-DenseNet," *In 2022 9th Iranian Joint Congress on Fuzzy and Intelligent Systems (CFIS)*, pp. 1-5: IEEE, 2022.

[41] K. Simonyan and A. Zisserman, "Very deep convolutional networks for large-scale image recognition," *arXiv*, 2014.

[42] C. Nicholson, "Evaluation metrics for machine learning—accuracy, precision, recall, and F1 defined," *ed: Pathmind. http://pathmind.com/wiki/accuracy-precision-recall-f1*, 2019.

V. Esmaeili received her B.S. degree in electrical engineering from the Azad University of Abhar, Iran, in 2015 and the M.S. degree in electrical engineering from the Azad University of Qazvin, Iran, in 2018. Since 2019, she has been working toward the Ph.D. degree in electrical engineering at the Tabriz University, Iran. Her research interests include the area of image processing, machine learning, and pattern recognition.

M. Mohassel Feghhi received the BS and MS degrees (with Honors) in electrical engineering from the Iran University of Science and Technology, Tehran, Iran, in 2006 and 2009, respectively, and the Ph.D. degree in electrical engineering from the College of Engineering, University of Tehran, Iran, in 2015. From 2007 to 2016, he held positions as a senior design engineer in the areas of communication systems design with several Communications Industries and Inc. Since 2016, he has been with the Faculty of Electrical and Computer Engineering, University of Tabriz, Iran, where he is now an associate professor. His current research interests include information theory, wireless communication networks, signal processing, machine learning, and optimization.